



# In-vitro and In-vivo Characterization of Methotrexate-loaded Liposomes for the Treatment of Psoriasis

Rinkee Verma<sup>1</sup>, Divya Sahu\*<sup>2</sup>, Mansi Sen<sup>3</sup>, Pankaj Bhardwaj<sup>4</sup>, Kamal Bareth<sup>5</sup>, Vikas Kumar Sahu<sup>6</sup>, Trilok Nath Patel<sup>7</sup>, Jhakeshwar Prasad<sup>8</sup>

<sup>1</sup>Rungta College of Pharmaceutical Sciences and Research, Nandanvan, Raipur - 492099, Chhattisgarh, India

<sup>2</sup>University Institute of Pharmacy, Pt. Ravishankar Shukla University, Raipur – 492010, Chhattisgarh, India

<sup>3</sup>RIT College of Pharmacy, Chhatauna Mandir Hasaud – 492101, Raipur, Chhattisgarh, India

<sup>4</sup>Shri Balaji College of Pharmaceutical Sciences, Sakti – 495689, Chhattisgarh, India

<sup>5</sup>DBM College of Pharmacy, Devraha – 495667, Chhattisgarh, India

<sup>6</sup>Kamla Institute of Pharmaceutical Sciences, Junwani – 490020, Bhilai, Chhattisgarh, India

<sup>7</sup>R. N. Dubey College of Pharmacy, Khorsi – 495556, Janjgir-Champa, Chhattisgarh, India

<sup>8</sup>Shri Shankaracharya College of Pharmaceutical Sciences, Junwani – 490020, Bhilai, Chhattisgarh, India

**Corresponding Author** – divyasahu5837@gmail.com

*(Received: 04 February 2024*

*Revised: 11 March 2024*

*Accepted: 08 April 2024)*

## KEYWORDS

Psoriasis;  
Methotrexate;  
Liposomes;  
Microneedles;  
In-vitro studies

## ABSTRACT:

Methotrexate (MTX) is a first-line drug in treating psoriasis because of its strong anti-proliferation and anti-inflammatory effects. However, systemic administration of MTX will lead to many side effects, such as gastrointestinal irritation, liver and kidney toxicity, etc. Herein, we developed liposome-loaded microneedles (MNs) system to improve transdermal efficiency, which was used to overcome the problems of low transdermal efficiency and poor therapeutic effect of traditional transdermal drug delivery methods. Hyaluronic acid (HA) was modified on the surface of MTX-loaded liposomes. The interaction of HA and CD44 could increase the adhesion of HA-MTX-Lipo to HaCaT cells, thereby promoting the apoptosis or death of HaCaT cells. Results indicated HAMTX-Lipo MNs could inhibit the development of psoriasis and reduce the degree of skin erythema, scaling, and thickening. The mRNA levels of proinflammatory cytokines such as IL-17A, IL-23, and TNF- $\alpha$  were decreased. The epidermal thickness and proliferative cell-associated antigen Ki67 expression were also reduced. Specifically, the expression of mRNA levels of proinflammatory cytokines was down-regulated. The MNs transdermal delivery of HA-modified-MTX liposomes provided a promising method for treating psoriasis.

## 1. Introduction

Psoriasis affects about 125 million people worldwide. As an immune-mediated chronic skin disease, psoriasis is characterized by excessive epidermal thickening and skin inflammation, most commonly in the elbow, knee, scalp, and back. The main risk factor for psoriasis is genetics, and dysregulation of homeostasis between the immune systems and the skin reservoir cells is the leading cause of psoriasis [1]. Most psoriasis administration methods are systemic, though systemic administration can lead to many side effects, low bioavailability, and poor patient compliance, thus affecting efficacy. Furthermore, with the high price of

targeted biological agents, patients' adherence is scarce and difficult to continue [2]. Methotrexate (MTX) was officially approved for the treatment of psoriasis by FDA in 1971, with a reasonable price and good therapeutic effect, and it is still the preferred drug for the treatment of psoriasis. MTX is activated by cytosolic folyl polyglutamate synthetase (FPGS) and inhibits dihydrofolate reductase (DHFR) in the form of polyglutamate (MTX-PGs), which inhibits DNA synthesis and exerts cytotoxic effects. MTX inhibits T and B lymphocytes, proinflammatory cytokine production, neutrophil and monocyte chemotaxis, and keratinocytes synthesizing DNA and inducing apoptosis



[3]. The current administration method available includes oral and injection. Still, unfortunately, liver first-pass effect and pharmacokinetic nonlinearity are characteristics of MTX oral administration route, which reduces its bioavailability and thus affects the efficacy. Meanwhile, the injection method is very inconvenient. It may cause pain, bleeding, and poor compliance of patients, and the medical waste generated will also bring the risk of disease transmission. Moreover, many side effects can be caused by systemic administration of MTX, including gastrointestinal disorders (such as nausea, vomiting, and diarrhea), hepatotoxicity, bone marrow dysfunction, dyspnea, anemia, and other side effects [4,5]. Local administration of MTX seems an effective way to avoid firstpass effects and systemic toxicity. Numerous studies have been conducted to improve transdermal results by changing MTX dosage forms (including microemulsions liposomes and nanoparticles etc.) or using electroporation, ion electroosmosis, ultrasound, and microneedles. Microneedles (MNs) is a novel transdermal drug delivery system. Drugs can be stored in micropores or be released directly into the dermis after penetrating the epidermis to produce local or systemic therapeutic effects through the vascular network in the dermis [6, 7]. What's more, keratinocytes, Langerhans cells (LC), dermal DC, and T cells, which are widely present in the skin, play a positive role in the immune regulation behavior of the skin. Hence, the advantages of percutaneous immunity are unique. In recent years, some studies have used the combination of MTX and microneedles to treat psoriasis. Hongyao Du et al. loaded MTX into HA-based dissolving MNs to deliver the drug locally in psoriasis, achieving a better therapeutic effect than oral administration. Duohang Bi et al. co-loaded methotrexate (MTX) and epigallocatechin gallate (EGCG) into ROS-responsive MNs to achieve anti-inflammatory and anti-proliferative effects in treating psoriasis, the coordination with other drugs to MTX load of functional scheme is also one of the application direction of MTX. Simultaneously, the construction of a nano-drug delivery system suited for MTX can bestow various therapeutic advantages of MTX [8]. Yong Zhou et al. synthesized a ROS-reactive MTX prodrug (MTX-TK-HA) with CD44-mediated active targeting of hyperproliferating keratinocytes. MTX-TK-HA/PLA-mPEG nano assemblies were

prepared to release MTX-TK-HA in response to ROS stimulation with CD44-mediated active targeting. Liposomes are small vesicles formed by the encapsulation of drugs in lipid-like bilayers [9]. It is often used in local or transdermal administration to effectively treat skin diseases because phospholipid molecules or nonionic surfactants on the surface of liposomes can diffuse to the cuticle and act as penetration promoters. The advantages of liposomes include extended drug release, sufficient drug stability, good biocompatibility, desirable targetability, and adequate loading ability of both hydrophilic and hydrophobic active ingredients [10]. Liposomes are easy to be modified, and are easy to be taken up by cells, which could further improve its targeting efficacy. Therefore, the combination of liposomes and MNs for local delivery of MTX has a broad prospect. As a polymorphic type I transmembrane glycoprotein, CD44 is widely expressed on the surface of mammalian cells, including epithelial cells, endothelial cells, leukocytes, fibroblasts, and keratinocytes [11]. The diversity of CD44 is determined by cell type-specific glycosylation and differential splicing of at least ten variable exons. CD44 protein overexpressed in the skin of inflammatory sites, especially in the epidermis of psoriasis, indicating its potential as a target for nano drug delivery systems to achieve localized drug accumulation in the skin. HA is the primary cell surface ligand of CD44, which is related to many biological effects: a key component of ECM tissue, immunomodulatory function, participation in various cellular processes, etc. [12,13]. Meanwhile, HA and CD44 are related to activating and regulating immune cell movement, apoptosis and immune tolerance. The interaction between CD44 protein and HA could regulate the keratinocytes (survival, cell-cell adhesion, proliferation, differentiation, migration, and epidermal barrier formation) and improve the abnormal epidermis. It plays a very crucial role in psoriasis. In this study, we fabricated MNs loaded with MTX-loaded liposomes with HA surface modification. MNs can deliver drugs to the dermis efficiently and painlessly across the epidermal barrier [14]. Simultaneously, the application of MNs loaded liposomes greatly improve the low bioavailability and decrease systemic toxicity of MTX. Loading MTX into liposome-loaded microneedles can improve targeted delivery efficiency and bioavailability



while playing a certain degree of sustained release [15]. HA was used to modify the liposome surface, which could interact with CD44 protein, promote the internalization of MTX, and stimulate immune cells in the skin. Then we investigated the liposome uptake before and after HA modification and the effect of different forms of MTX on the apoptotic. Also, the therapeutic efficacy of this system was assessed by the pathological state of the diseased skin and the expression of the inflammatory cytokines *in-vivo* [16, 17].

## 2. Materials and methods

Methotrexate hydrate (MTX) was purchased from Sigma-Aldrich, Mumbai (Maharashtra, India). Hyaluronic acid (MW = 150 kDa) was purchased from Sigma-Aldrich, Mumbai (Maharashtra, India). Annexin V-FITC/PI Apoptosis Detection Kit was purchased from Loba Chemie Pvt. Ltd. Mumbai (Maharashtra, India). Promega GoScript Reverse Transcription System Kit was purchased from Loba Chemie Pvt. Ltd. Mumbai (Maharashtra, India). SYBR green mix was purchased from Sigma-Aldrich, Mumbai (Maharashtra, India). The TRIzol cell lysate was purchased from Sigma-Aldrich, Mumbai (Maharashtra, India).

### Animals

BALB/c mice (8 ~ 10 weeks, 20 ± 2 g) were supplied by the Columbia Institute of Pharmacy, Raipur (Chhattisgarh, India). All studies were reviewed and approved by the Institutional Animal Ethics Committee (IAEC) Government of India.

### Methods

#### Preparation of liposomes

The composition of the resulting liposomes was shown in Table 1. The preparation process was as follows: Hydrogenated soybean lecithin (HSPC), phosphatidyl ethanolamine (PE), and cholesterol (Chol) were dissolved in the organic phase as the oil phase and PBS (0.1 M, pH = 7.4) as the aqueous phase. The volume ratio of the organic phase to the aqueous phase was 3:1. After mixing the two steps, the ice bath probe was ultrasonic (power 150 W) for 5 min [18]. The w/o emulsion was formed, and the semi-solid gel was obtained by rotating under reduced pressure at 30 °C for

30 min. PBS was added and continued spinning to remove residual organic solvents. Finally, the ice bath probe was ultrasonic for 5 min, and the uniform liposome solution was extruded by liposome extruder. HA was modified on the surface of liposomes according to the reported method [19, 20]. The prepared liposome solution was centrifuged at 186,000 g to obtain liposome precipitation and placed for 1 h at 4 °C. Equal masses of HA, EDC, and NHS were dissolved in purified water, and pH was adjusted to 4 with hydrochloric acid. After 2 h incubation (37 °C, rotational speed 300 rpm), the solution (500 µL) was mixed with 0.1 M borate buffer (pH = 9.500 µL) and blank liposomes (10 mg). The pH of the mixture was adjusted to 8, and the mixture was incubated for 24 h (37 °C, 300 rpm) to obtain HA-Blank-Lipo. MTX was loaded into HA-modified liposomes using the "small volume incubation (SVI)" method (Xu et al., 2014). In brief, MTX solution (1.5 mg of MTX dissolved in PBS pH 7.4) was added to 10 mg of liposomes, vortex mixed for 3 min, and incubated at 60 °C for 3 h to investigate the effect of the volume of added PBS on liposomes [21,22].

#### Determination of particle size, PDI, potential (ζ), and EE of liposomes

The particle size, PDI, and potential (ζ) of liposomes were measured by DLS particle size meter at 25 °C and measured three times in parallel. 1 mL of liposomes was placed in the inner tube of a 50-kDa ultrafiltration tube and centrifuged in a superfast centrifuge for 30 min (4 °C, 8000 rpm) to obtain a free MTX solution, which was diluted and measured with a UV spectrophotometer (303 nm wavelength). Entrapment Efficiency (EE%) was calculated according to Eq. (1):

$$EE \% = (C1 - C2) / C1 \quad (1)$$

In the equation, C1: total concentration of MTX, C2: concentration of free MTX.

#### Morphological characterization of liposomes

The tested sample was dropped onto the copper mesh and pretreated, after which the sample morphology was observed under TEM. Then the prepared liposomes were loaded into the MNs, and the released liposomes were collected after dissolving at the tip of the MNs. The morphological integrity of the liposomes was observed under TEM.



### Stability of liposomes

The liposomes were stored at 4 °C. After 0, 7, and 15 days of storage, the particle size and PDI of liposomes were measured to evaluate the stability of the preparation.

### MTX release in-vitro

PBS buffer pH 7.4 (0.01 M) was used as the medium for the *in vitro* release experiment. A dialysis bag (14 KDa) containing MTX, MTX-Lipo, and HA-MTX-Lipo was transferred to a beaker (containing 100 mL of the release medium, and the dialysis bag was completely immersed in the release medium). The beaker was placed in a full-temperature shaking incubator (37 °C, 100 rpm), and the *in vitro* release experiment was started. At predetermined time intervals, 1 mL samples were taken to calculate the release rate, and an equal volume of PBS buffer was added to ensure a constant volume of the release medium. MTX content was determined using a microplate reader (303 nm wavelength).

### Cytotoxicity test

Cytotoxicity was detected by mouse embryonic fibroblasts (L929) and human immortalized keratinocytes (HaCaT). The cells were added to a 96-well plate at a specific density (5000–10,000/well, 100 µL per well), and 100 µL of different concentrations of drugs were added to each well after the cells were covered with the bottom of the well. After 24 h, it was removed and 20 µL MTT (5 mg/mL) was added to each well. After 4 h, the medium was carefully discarded, and 150 µL DMSO was added. The absorbance value of each well was measured, and the cell survival rate% was calculated according to Eq. (2):

$$\text{Survival rate of cells \%} = (A_s - A_b) / (A_c - A_b) \times 100$$

In the equation,  $A_s$ : absorbance value of experimental group (including cell, drug, medium, MTT, DMSO);  $A_b$ : absorbance value of blank group (including medium, MTT and DMSO);  $A_c$ : Absorbance value of control group (including cell, medium, MTT, DMSO, without drug).

### Cell uptake experiment

Rhodamine B (Rh B), a water-soluble fluorescent indicator, was used to simulate homogenous MTX.

HaCaT cells were seeded onto confocal cell culture dishes at a  $1.5 \times 10^5$  cells/dish density and cultured for 24 h. After 22 h of culture, HaCaT cells were treated with 0.2 mg/mL HA (50 µL) for 2 h in advance. After 24 h of culture, the old medium was replaced with 1.5 mL of FBS-free DMEM medium containing Rh B-Lipo and HA-Rh B-Lipo, respectively, with Rh B concentrations of 20 µg/mL. After 8 h incubation in a constant temperature incubator, cells were fixed with 500 µL 4 % paraformaldehyde and stained with 500 µL DAPI solution (5 mg/mL). Finally, the film was sealed to avoid light, and the uptake was observed and photographed under a laser confocal microscope.

### Apoptosis experiment

Apoptosis was verified by Annexin V-FITC/PI kit. HaCaT cells were inoculated into 6-well plates at a density of  $2 \times 10^5$  per well. After the adherent growth of cells reached 70–80 % density, different test reagents were added to make the final concentration of MTX 30 µg/mL. The final concentration of LPS was 100 ng/mL. The culture was continued for 24 h. The experimental groups are as follows:

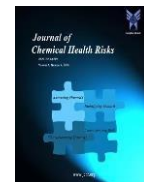
Control group: HaCaT The experimental group:

- (1) HaCaT + LPS
- (2) HaCaT + LPS + HA
- (3) HaCaT + LPS + MTX
- (4) HaCaT + LPS + MTX-Lipo
- (5) HaCaT + LPS + HA-MTX-Lipo

After 24 h, cells were digested with 0.25 % trypsin without EDTA, blown and centrifuged, collected, resuspended with binding buffer, and incubated with Annexin V-FITC and PI in the dark for 15 min. After staining and incubation, 400 µL of binding buffer was added to each tube, mixed and then detected by Flow cytometry and analyzed by Flow Jo.

### Cytokine detection by PCR

HaCaT cells were lysed with TRIzol, the cell lysate was collected, and 200 µL trichloromethane was added, mixed, and then stood for stratification, and centrifuged (12,000 rpm, 15 min, 4 °C). The upper RNA solution was added to 500 µL isopropanol, mixed, and centrifuged. After discarding isopropanol and washing with 70 % (v/v) ethanol, RNA was extracted from HaCaT cells. Then the RNA concentration was adjusted to 1000 ng/µL according to the RNA concentration of



the samples. The cDNA was constructed by Promega GoScript Reverse Transcription System, and the concentration of single-stranded DNA was determined. Samples were added to a 96-well plate, and SYBR green mix was used as dye. The SYBR Green method was selected for qPCR. The data was analyzed and processed by comparative CT.

### Preparation and Characterization of microneedles

The HA with a concentration of 12.5 % (w/v) was placed in the female mold, 150  $\mu$ L HA was inserted into each microneedle mold, centrifuged for 30 min to remove the bubbles, scraped off the excess HA, and dried in a vacuum desiccator to obtain the tip part of the MNs. The MNs tip material could lose water and contract during vacuum drying, forming holes at the base of the tip. To prepare drug-loaded microneedles, the drug in the form of dry powder was filled into the holes created by vacuum drying of the MNs tip. Each mold was filled with 1 mg of dry powder drug, and an external force was applied to fill the holes with the drug and the excess drug was scraped away. Finally, the backing part was prepared: After vacuum drying for 12 h, 150  $\mu$ L 7.5 % (w/v) HA was added to the surface of the mold and centrifuged at a reduced speed for 30 min (*i.e.*, horizontal centrifugation at speeds of 3000, 2500, 2000, 1500, 1000 and 500 rpm for 5 min each) to form a uniform MNs backing layer. The dissolving microneedles were made when it was completely dried. The mechanical properties of MNs and the critical buckling force of MNs were investigated using Texture Analyser's compression mode. The critical buckling force of MNs before fracture was obtained by the relationship between the force and the displacement. The morphology of HA MNs was observed by scanning electron microscopy (SEM). The MNs sample was plated with a thin layer of gold (several nanometers thick) to enhance the electrical conductivity of MNs and reduce the charge effect in the shooting, which was conducive to obtaining high-quality photos. The MNs were mounted on the sample holder for observation and taking photos. The skin of mice was placed on a plane and pressed with MNs for 1 min. The skin of the puncture surface was placed down on the bottom surface of the trapezoidal prism of optical coherence tomography (OCT). The state of MNs penetrating the skin was observed and photographed by OCT. The

dried MNs were inverted on a pre-perforated polyethylene (PE) film with only the needle exposed to PBS buffer (pH 6.5, mimicking skin pH). The dissolution experiment of HA MNs was carried out in a full temperature shaking incubator (37 °C, 50 rpm). MNs were removed every once in a while, and the residual water on the surface of MNs was absorbed by filter paper. The dissolution of MNs was observed under a microscope and recorded by taking photos.

### Microneedles puncture experiment

The isolated skin of Balb/c mice was used to investigate the performance of skin piercing. Clean skin was laid flat on the table, and HA MNs were pressed to pierce the skin for about 1 min. The skin pinholes were treated with 0.4 % trypan blue solution, and the excess trypan blue solution was washed away after 5 min. The puncture effect of MNs was observed and photographed. After the mice were anesthetized with isoflurane, the back was depilated, and the MNs patch was applied to the hairless skin of the back for 1 min. Finally, the healing process of the mouse skin was photographed. The skin irritation of MNs was determined by the Draize skin response criteria rating scale (Ngo and Maibach, 2010). 8 Balb/c mice were anesthetized and shaved. MNs were applied to the glabrous skin for 1 min. After 1 h, 24 h, and 72 h, their back erythema and scab were scored and the total score was calculated according to Eq. (3).

$$PII = \frac{\sum(1, 24, 72 \text{ h})}{(\text{Number of mice} \times \text{number of observations})} \quad (3)$$

### In-vitro transcutaneous drug release assay with microneedles

*In-vitro* percutaneous permeation experiments were performed using a classical Franz transdermal diffusion cell. The isolated skin of Balb/c mice was collected, and the subcutaneous adipose tissue was removed. The skin was immersed in normal saline for 1 h, and the excess water was blotted out with filter paper. The experiments were divided into four groups: MTX MN, MTX-Lipo MN, MTX Hydrogel, and MTX-Lipo Hydrogel. It was ensured that each assembly was loaded with approximately 100  $\mu$ g of MTX. Each experiment was repeated three times. The MTX MN and MTX-Lipo MN were inserted into the central region of the isolated skin, while the MTX hydrogel and MTX-Lipo hydrogel



made direct contact with the central area of the isolated skin. The skin was fixed to the receiver compartment of the diffusion cell. To mimic *in-vivo* conditions, 7.2 mL of pH 7.4 PBS was used as the receiver solution (600 rpm,  $32\pm 1$  °C). The release medium was collected at 0, 1, 2, 3, 6, 9, 12, 24, 36, 60 and 72 h. Each collection of the medium (600  $\mu$ L) was supplemented with an equal volume of fresh release medium. The sample solution was filtered through a 0.2  $\mu$ m filter and absorbance was measured at a UV wavelength of 303 nm.

### Establishment of psoriasis mouse model

Balb/c mice were organized into groups, with 8 mice allocated to each group. The dose of the MTX group was about 10  $\mu$ g per dose. The groups are as follows:

- (1) Normal control group (Normal)
- (2) Psoriasis inflammation model group (Model)
- (3) Blank microneedles administration group (Blank MNs)
- (4) MTX microneedles administration group (MTX MNs)
- (5) MTX liposome microneedles administration group (MTX-Lipo MNs)
- (6) HA modified MTX liposome microneedles administration group (HA-MTX-Lipo MNs)
- (7) Clobetasol propionate cream group (CP)
- (8) MTX injection group (MTX iv.)
- (9) MTX gavage group (MTX po.)

After one week of adaptive feeding, the back hair of the mice was shaved with a shaving machine. Except for the control group, IMQ cream was applied at a dose of 25 mg/cm<sup>2</sup> once a day for 7 days to establish psoriatic inflammation.

### Psoriasis area and severity index (PASI) score

PASI score was used as an evaluation index in the psoriasis model. The erythema, scale, and thickening of the skin on the back of mice were scored (0, no apparent lesions; 1, mild; 2, moderate; 3, obviously; 4, very obvious). The sum of erythema, desquamation, and skin thickening scores (0 to 12) was used to assess the severity of inflammation. From the date of molding, the scores were scored once a day for 8 consecutive days. On day 8, the back skin of all groups was observed and photographed.

### H & E staining

On the 8th day, Balb/c mice were sacrificed by neck removal and dissected. The skin of the psoriasis model was taken and fixed in a 4 % paraformaldehyde fixation solution for 24 h. The skin was dehydrated by different concentrations of ethanol (70 %, 1 h; 85 %, 1 h; 95 %, 1 h; 100 %, 3 h), and then the skin was put into xylene to make it transparent. The skin was made into 4  $\mu$ m thick skin paraffin sections and subjected to H&E staining. Finally, the sections were dehydrated, transparent and sealed, placed under a microscope, and photographed. 6 different sites were randomly selected on H&E-stained tissue sections and photographed with panoramic scanner software, and the epidermal thickness was measured by Image J software.

### Immunohistochemical (IHC) analysis

For IHC analysis, paraffin sections of skin from the psoriasis model were dewaxed with xylene and hydrated with ethanol gradient. Ki67 was used to identify nuclear antigens present in proliferating cells and thus reflect the proliferation rate of keratinocytes. Antigen repair of Ki67 and CD44 (citrate buffer, pH 6.0, 100 °C, 10 min) was followed by blocking treatment with 3 % H<sub>2</sub>O<sub>2</sub> for 10 min to block nonspecific antibody binding. The slides were incubated for 60 min (in Tris buffer containing 1 % BSA at 25 °C). After washing with PBS, the slides were incubated with primary antibody (Abs) overnight at 4 °C. Horseradish peroxidase (HRP) labeled secondary antibody was added drop, the reaction was performed for 30 min, and then diaminobidine (DAB) was reacted. After the slides were counterstained with hematoxylin, the sections were put into different concentrations of ethanol (75 %, 5 min; 85 %, 5 min; 100 %, 5 min, 2 times), xylene I for 5 min, dehydrated and transparent, and the slices were sealed with neutral gum. Finally, they were observed under a light microscope and micrographs were taken.

### Mouse spleen index

On the 8th day of modeling, Balb/c mice were weighed; their body weight was recorded, and then sacrificed by necking. Then the humanely killed mice were dissected, and their spleens were taken, weighed, and recorded. Finally, the spleen index of mice was calculated according to Eq. (4).



Spleen index = Spleen mass/Total mouse mass (4)

### Detection of cytokines in mice skin

Firstly, 100 mg of skin washed from the psoriasis model of Balb/c mice was cut into pieces and placed in homogenate tubes. Several magnetic beads and 1 mL TRIzol were added into the homogenization tube, and then placed in the tissue homogenizer after the lid was closed for homogenization (6500 rpm, 30 s, 3 times). After the skin tissue was homogenized entirely, it was allowed to stand for 5 min, and the supernatant was removed by centrifuge (3500 rpm, 1 s) and transferred to an EP tube. The method of detecting cytokines in HaCaT cells in 2.3.9 was used to extract RNA and construct cDNA successively. Finally, the sample was added to the 96-well plate, and SYBR green mix was

used as the dye with the primers. The instrument and software were opened, and the SYBR Green method was selected for qPCR. The data were analyzed and processed by comparative CT.

### Statistical analysis

GraphPad Prism was used for statistical analysis, and a one-way analysis of variance was performed. The experimental results were expressed as mean  $\pm$  standard deviation. P value below 0.05 ( $P < 0.05$ ) was considered statistically significant. Compared with the control group:  $+P < 0.05$ ;  $++P < 0.01$ ;  $+++P < 0.001$ ;  $++++P < 0.0001$ ; Compared with the model group:  $*P < 0.05$ ;  $**P < 0.01$ ;  $***P < 0.001$ ;  $****P < 0.0001$ .

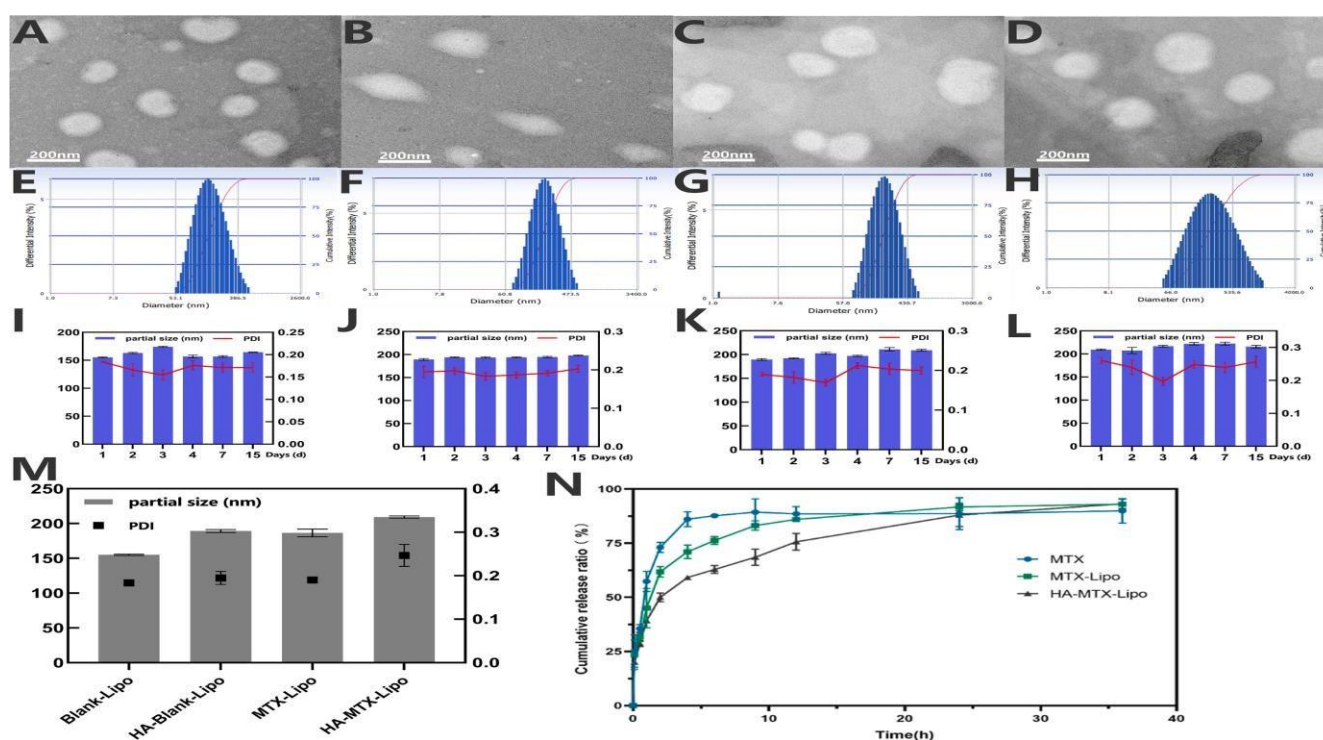


**Fig. 1.** (A, B, C, D) TEM image of Blank-Lipo, HA-Blank-Lipo, MTX-Lipo, and HA-MTX-Lipo, scale bar: 200 nm; (E, F, G, H) Intensity distribution of Blank-Lipo, HBlank-Lipo, MTX-Lipo, and HA-MTX-Lipo; (I, J, K, L) Particle size and PDI stability of Blank-Lipo, HA-Blank-Lipo, MTX-Lipo, and HA-MTX-Lipo ( $n = 3$ ); (M) Particle size and PDI of Blank-Lipo, HA-Blank-Lipo, MTX-Lipo, and HA-MTX-Lipo ( $n = 3$ ); (N) *In vitro* MTX release of three preparations (pH 7.4 PBS,  $n = 3$ ).

## 3. Results and discussion

### Characterization of drug-loaded liposomes

Phospholipids are amphoteric substances, containing hydrophilic and oleophilic groups, which are the main chemical components of liposomes. Hydrogenated soybean phospholipid (HSPC) and phosphatidyl

ethanolamine (PE) are commonly used as phospholipid materials to prepare liposomes. The presence of amino groups in PE provides conditions for subsequent amide reactions with carboxyl groups on HA. As seen from the TEM images in Fig. 1 (A, B, C, D), Blank-Lipo, HBlank-Lipo, MTX-Lipo, and HA-MTX-Lipo are



large single-chamber liposomes with good dispersion and no obvious aggregation and fusion phenomenon. Blank-Lipo and MTX-Lipo vesicles were uniform and spherical, with a particle size of less than 200 nm, similar to the measurement result of the Malvern particle size meter Fig. 1 (E, G). The modification of HA will increase the particle size of liposomes, and the particle size of HA-blank-Lipo and HA-MTX-Lipo are about 200 nm, Fig. 1 (F, H), which may be caused by the coupling of HA on the surface and the expansion of hydrated HA molecules. HA contains hydroxyl and carboxyl groups, which form helical intermolecular and intramolecular hydrogen bonds when dissolved in aqueous solution. This helical conformation makes HA highly absorbent (Stern et al., 2006), thus making the liposomes as a whole larger.

The stability investigation experiment of Blank-Lipo, HA-Blank-Lipo, MTX-Lipo, and HA-MTX-Lipo Fig. 1 (I, J, K, L) showed no obvious aggregation and condensation phenomenon of the four kinds of liposomes within 15 days, indicating that the prepared liposomes were very stable in the PBS environment with pH 7.4. In addition, the loading of MTX into liposomes has little effect on its morphology, particle size and stability, which proves that the liposomes prepared in this way are excellent carriers of MTX. The *in vitro* release results of various MTX preparations were shown in Fig. 1(N). At the 4 h,  $86.06 \pm 3.45$  % of the MTX group had been released, and the free MTX was quickly released in the dialysis bag of 14 KDa. At this time, the release rate of the MTX-Lipo group was  $71 \pm 3.07$  %, indicating that the carrier form of liposomes played a certain degree of sustained release. The cumulative release rate of the HA-MTX-Lipo group was the lowest ( $59.14 \pm 0.42$  %). The HA modified on the surface of liposomes formed a gel network that prevented MTX diffusion into the release medium through the phospholipid membrane and HA gel layer. At 9 h, the cumulative release rate of MTX-Lipo group reached  $83.17 \pm 2.15$  %, which was not

achieved until about 24 h later in HAMTX-Lipo group. This facilitates MTX delivery to the skin in the form of HA-MTX-Lipo when administered locally.

#### **In vitro cell assay**

MTX inhibits DNA synthesis and induces apoptosis in keratinocytes [23]. Lipopolysaccharide (LPS), a key structural element of the outer membrane of Gram-negative bacteria, triggers the immune response of cells by activating Toll-like receptors (TLRs), inducing the secretion of pro-inflammatory cytokines and promoting cell proliferation. Therefore, LPS was pre-added to HaCaT cells to mimic keratinocytes under the inflammatory skin of psoriasis. The toxicity of different MTX preparations on HaCaT cells pretreated with LPS was shown in Fig. 2 (A, B, C). With the increase of MTX concentration, the cell viability gradually decreased. When the concentration of MTX was 300  $\mu\text{g/mL}$ , the half lethal dose was reached. Among them, HA-MTX-Lipo showed the most robust activity [24, 25]. The cellular uptake of liposomes was qualitatively analyzed by CLSM, and the experimental results were shown in Fig. 2(D). The experimental groups were divided into Rh B-Lipo, HA-Rh B-Lipo and HA pretreated Rh B-Lipo (HA + Rh B-Lipo), to study the effect of liposome surface HA modification on cell uptake. The cellular uptake capacity of Rh B-Lipo pretreated with HA was weaker than that of HA-modified liposomes, indicating that HA modified on the surface of liposomes could significantly improve the cellular uptake capacity, rather than a simple mixed effect, which may be related to the endocytosis mediated by CD44, the receptor of HA. Fig. 2(E) showed the scatter plot of apoptosis of HaCaT cells after incubation with MTX preparations for 24 h. In addition to the control group, other groups were pretreated with LPS. The late apoptosis was mainly induced by MTX, but the effect on early apoptosis was small [26, 27].

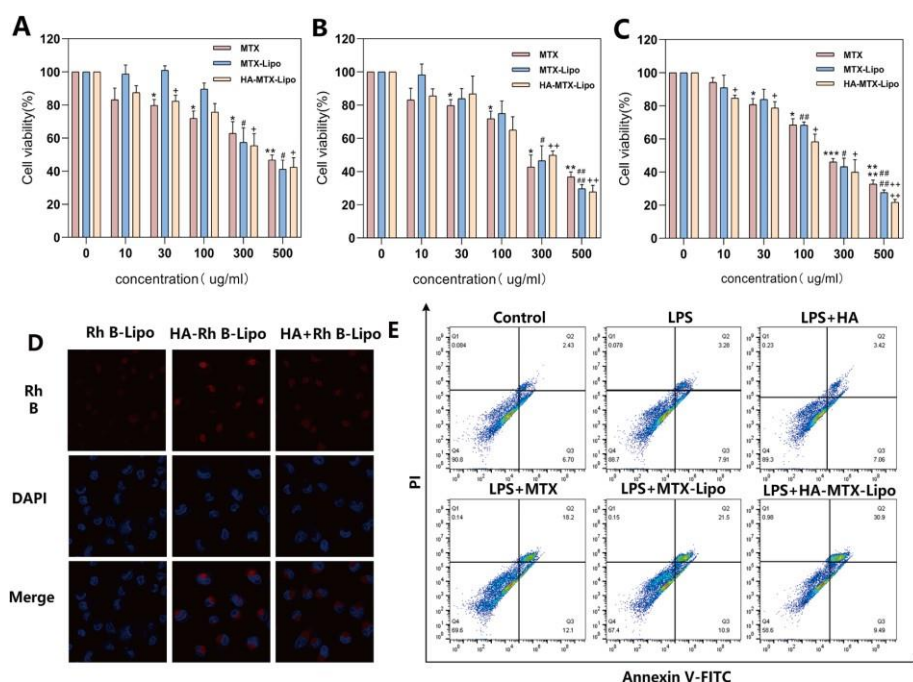


**Fig. 2.** Viability of (A) L929 cells, (B) HaCaT cells, (C) LPS-pretreated HaCaT cells at different concentrations ( $n = 3$ ); (D) The uptake of Rh B by HaCaT cells when coincubated for 8 h; (E) Scatter plot of apoptosis of HaCaT after incubation with MTX preparation.

The percentage of apoptosis (Q1 + Q2) in control group, LPS group, HA group, MTX group, MTX-Lipo group, and HA-MTX-Lipo group were 9.13 %, 11.19 %, 10.48 %, 30.30 %, 32.4 %, and 40.39 %, respectively. The results showed that apoptosis was most significantly affected by HAMTX-Lipo group, which was attributed to the increased secretion of inflammatory factors and CD44 on HaCaT cells after LPS treatment. However, the surface modification of HA increased the adhesion to HaCaT cells, increased the internalization of MTX, played its role in inhibiting the DNA of HaCaT cells, and promoted the apoptosis of HaCaT, which was consistent with the results of the cytotoxicity assay. The apoptosis rate of the control group, LPS group, and HA group was about 10 %, which may be caused by the natural apoptosis of HaCaT rather than the effect of the drug, or the apoptosis induced by LPS and HA reagent was very little.

### Cytokine results of HaCaT cells

The pathogenesis of psoriasis is related to the dynamic interaction between various cells and cytokines. The imbalance of immune homeostasis in psoriasis skin produces pro-inflammatory cytokines, including

interleukin-17 (IL-17), IL-1 $\beta$ , IL-23 and tumor necrosis factor- $\alpha$  (TNF- $\alpha$ ), and at the same time causes keratinocytes to produce chemokines, antimicrobial peptides and cytokines, which in turn aggravates the inflammatory response [28, 29]. TNF- $\alpha$  promotes keratinocyte secretion of IL-8. IL-8 recruits neutrophils, which then induces keratinocyte proliferation and psoriatic lesions [30]. IL-22 and IL-17 promote the proliferation of keratinocytes and lead to psoriatic lesions. In addition, IL-17 acts synergistically with IFN- $\gamma$  to induce keratinocytes to secrete cytokines such as IL-6 and IL-8, which affect the normal proliferation and apoptosis of psoriatic keratinocytes [31, 32]. Psoriasis is also exacerbated by IL-1 $\beta$  by promoting IL-17 secretion from  $\gamma\delta$ T cells. As shown in Fig. 3, the relative mRNA levels of proinflammatory cytokines TNF- $\alpha$ , IL-23, IL-6, IL-1 $\beta$  and IL-17A in HaCaT cells after LPS stimulation for 24 h were significantly higher than those in the normal control group ( $P < 0.0001$ ). After treatment with HA-MTX-Lipo, the expressions of TNF- $\alpha$ , IL-23, and IL-17A were not significantly different from those of the control group ( $P > 0.05$ ). Compared with the control group, the expression levels of IL-6 ( $P < 0.001$ ) and IL-1 $\beta$  ( $P < 0.05$ ) in the HA-MTX-Lipo

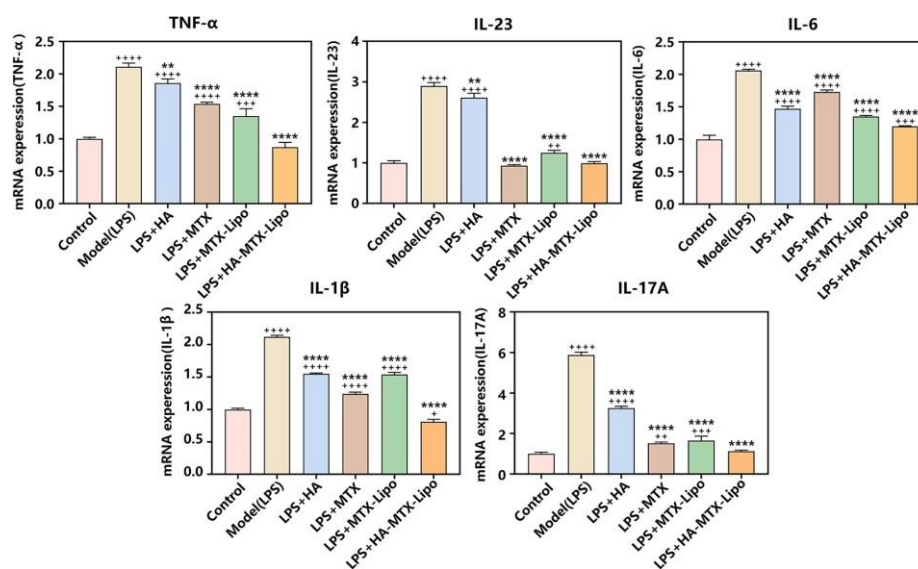


treatment group were still different. In general, the expression level of inflammatory factors in HaCaT cells stimulated by LPS was inhibited to a certain extent by HA-MTX-Lipo preparation. It can be seen that HA-MTX-Lipo preparation has the potential to impede the development of psoriasis by inhibiting HaCaT cells and subsequently inhibiting the expression of inflammatory cytokines [33, 34].

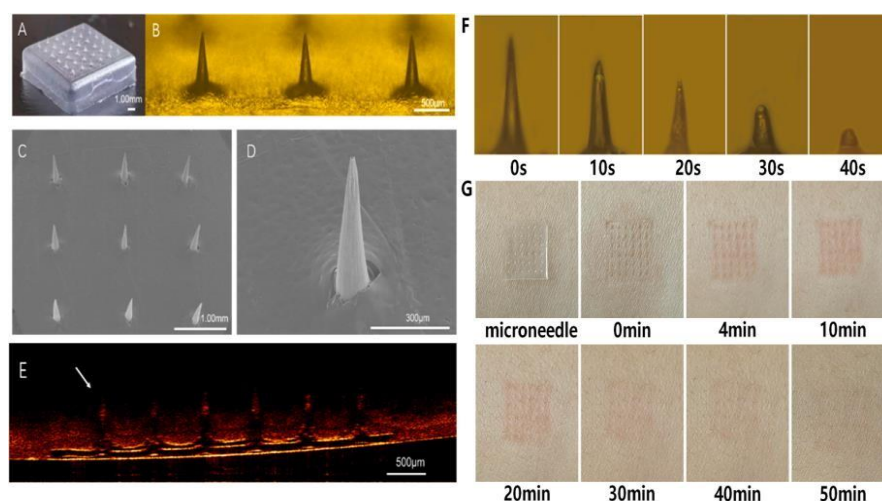
### Characterization of microneedles

Figure S3 showed the force-displacement curve of a single microneedle when HA MNs tip concentration was 12.5 % (w/v), and backing concentration was 7.5 % (w/v). When the probe of the texture meter contacted the tip of the MNs, the force began, the downward distance was 0.23 mm, the critical buckling force of the MNs was 0.23 N, and then a plateau period of almost constant force was formed. The default force required to penetrate the skin was  $3.596 \times 10^{-4}$  N [35], so the prepared MNs were sufficient to support penetration. Fig. 4(A) showed the MNs photographed by the camera, a square shape with an area of  $1 \text{ cm} \times 1 \text{ cm}$  and a  $6 \times 6$  array, with 36 conical MNs, and the spacing between needles was about 1 mm. Fig. 4(B) was an image taken under an ordinary light microscope. It can be seen from the figure that the needle is smooth and sharp, without bending or buckling, and the height is

consistent, so the backing is relatively uniform. Fig. 4 (C, D) showed SEM images of a  $3 \times 3$  MNs array and a single microneedle, respectively, where more microscopic MNs states can be observed: the needle length was about 500  $\mu\text{m}$ , the bottom diameter was 140  $\mu\text{m}$ , the tip diameter was 12  $\mu\text{m}$ , and the spacing of the needles was 1 mm. Therefore, the HA MNs prepared by the two-step method had a sharp tip, smooth surfaces, the same shape and length, and good homogeneity. The OCT image of the skin punctured by MNs was shown in Fig. 4(E). Six pinholes were visible, formed after single-row microneedle puncture, and the points indicated by arrows were the pits formed after needle puncture. It can be seen that the prepared MNs had good mechanical properties, and the MNs can be penetrated the skin. To verify the solubility of HA MNs, MNs were inverted on a perforated PE film, and the tip was exposed to PBS buffer pH 6.5. The dissolution process of HA was shown in Fig. 4(F). Before MNs met water, the needle body was smooth, and the needle was sharp. When the tip of the MNs needle was touched with water, the needle immediately absorbed water and collapsed, and slowly dissolved. After 40 s, the MNs dissolved completely. In conclusion, when the HA MNs with excellent solubility were pierced into the skin, the water in the skin could be rapidly absorbed, and the loaded drug could be quickly dissolved and released.



**Fig. 3.** Effects of different formulations on TNF- $\alpha$ , IL-23, IL-6, IL-1 $\beta$  and IL-17A expression levels of LPS-irritated HaCaT cells ( $n = 3$ ).



**Fig. 4.** Appearance and morphology of microneedles. (A) optical photo (scale bar: 1.00 mm); (B) microscope image (scale bar: 500  $\mu\text{m}$ ); (C) SEM image of  $3 \times 3$  microneedle array (scale bar: 1.00 mm); (D) SEM image of single microneedle (scale bar: 300  $\mu\text{m}$ ); (E) OCT image of skin after MNs puncture (scale bar: 500  $\mu\text{m}$ ); (F) Dissolution process of HA MNs; (G) Images of skin recovery after MNs piercing skin.

The HA MNs were placed on the skin for skin puncture experiment. After the MNs were pressed for 1 min, the MNs were removed, and its recovery condition was observed and photographed by camera, as shown in Fig. 4(G). When the MNs were removed,  $6 \times 6$  microholes were visible, and there were faint edge indentations, indicating that the tip of the MNs needle had been fully penetrated into the skin. With time, the micropores gradually disappeared, and the reddening first deepened and then faded, and the reddening was most evident at about 10 min. At 30 min, the pinhole was blurred and invisible, but still red. At 50 min, the skin recovered completely without pinholes and redness. The above results indicated that HA MNs with little damage to skin and no serious inflammation, were relatively safe. The skin irritation of HA MNs was evaluated by the Draize Skin response scale. Eight Balb/c male mice were selected and numbered respectively. After MNs were applied to the back of the mice, erythema and scab on the back were observed and scored. It can be seen from Table 2 that at 1 h after removing MNs, except mice A, E, and G still had very slight erythema. All the other mice had wholly recovered, and this result was also consistent with the skin recovery time after HA MNs insertion in Fig. 4(G). According to Formula 3, the final score was 0.125, meaning that HA MNs coating had no irritation to the skin of mice and could be used safely.

#### Effect of MNs in vitro percutaneous drug release assay

The liposomes can still maintain their intact morphology and the intact structure of large single-compartment liposomes after loading into the microneedles (Figure S4). Therefore, MTX-Lipo loading into MN can be considered for further *in vitro* transdermal release experiments. Fig. 5 showed that the MTX MN group had the fastest transdermal diffusion rate and can release  $50 \mu\text{g}/\text{cm}^2$  MTX in 24 h, which may be due to the microneedles penetrating the skin and directly delivering the drug into the receiving cell. However, in the MTX-Lipo MN group, the release rate of MTX into the receiving solution was decreased due to the liposome drug delivery form. Transdermal experiments were performed for 24 h, and the retention of MTX in the skin of the MTX MN group and the MTX-Lipo MN group was  $19.83 \pm 0.78 \mu\text{g}/\text{cm}^2$  and  $25.33 \pm 1.04 \mu\text{g}/\text{cm}^2$ , respectively. Compared with microneedle-mediated transdermal drug delivery, the transdermal diffusion rate of hydrogel drug delivery was significantly lower, probably due to the poor hydrophilic nature of MTX, which led to a lower penetration efficiency of the stratum corneum. The transdermal penetration of the MTX hydrogel group was still less than  $50 \mu\text{g}/\text{cm}^2$  at 72 h. The lower transdermal penetration of the MTX hydrogel group compared with the MTX-Lipo hydrogel group may be due to the flexibility and fluidity of the bilayer

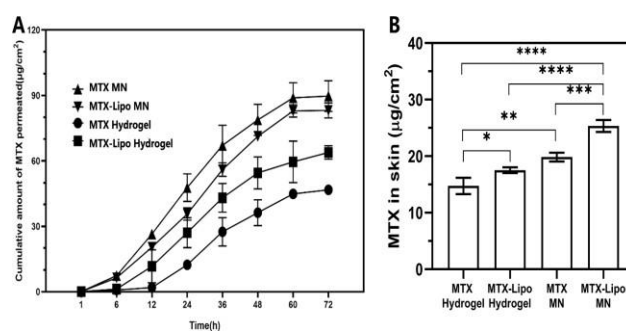


membrane of the liposomes, which act as a penetration enhancement, allowing the drugloaded liposomes to fuse with the skin and penetrate the skin more easily. At 24 h, the retention of MTX in the MTX hydrogel group and the MTX-Lipo hydrogel group was  $14.73 \pm 1.46 \mu\text{g}/\text{cm}^2$  and  $17.50 \pm 0.50 \mu\text{g}/\text{cm}^2$ , respectively.

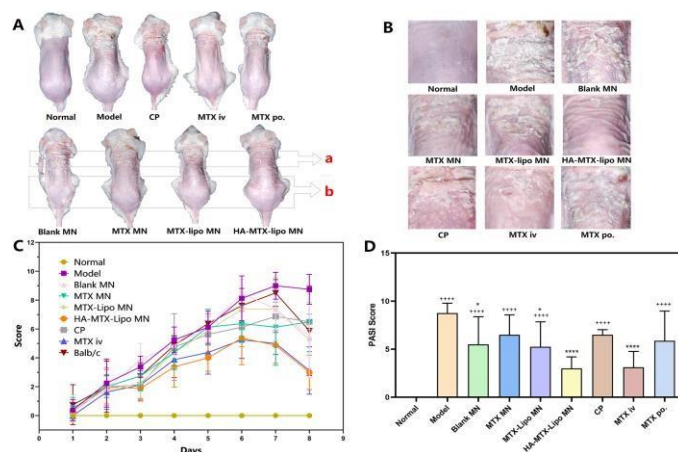
#### Degree of skin lesions in a mouse model of psoriasis

Fig. 6(A) showed the skin condition on the back of mice on the 8th day of IMQ modeling. The upper part of the back was the position where IMQ was applied every day for modeling, and the lower part was where microneedles group was used. Fig. 6(B) was the locally enlarged view of the molding place. In the control group, the skin was dark purple, smooth, without erythema, scaling, and thickening. In contrast, the model group had more white scales, skin thickening,

redness, and scab in the inflammatory wound. The scale of MTX po, Blank MNs, and MTXLipo MNs groups was reduced compared with the model group, but the effect was not noticeable. The scale and thickening of CP group and MTX MNs group were significantly improved. However, erythema still existed, indicating that these two groups had inhibited the development of psoriasis model to a certain extent. MTX iv and HA-MTX-Lipo MNs groups showed the best therapeutic effect, with few scales, erythema and skin relaxation. Except for the control group without IMQ, the other groups were smeared with the same amount of IMQ every day for modeling, and the treatment was carried out on the third, fifth, and seventh days. It can be seen from Fig. 6(C) that the PASI score of the model group was the highest.



**Fig. 5.** (A) Transdermal release of MTX ( $n = 3$ ); (B) The cumulative amount of MTX in the skin during the 24 h transdermal release experiment ( $n = 3$ ).



**Fig. 6.** (A) On the 8th day, the erythema, scaling and thickening of the back skin of the mice in each group (a: Psoriasis model site, b: MNs administration); (B) Enlarged images of skin of each group of mice on day 8; (C) Total PASI score of skin at mice models treated with various formulations ( $n = 8$ ); (D) Total PASI score of skin in mice model at day 8 ( $n = 8$ ).



The total PASI score on the eighth day was shown in the Fig. 6 (D). Compared with the normal group, the PASI scores of all the other groups were significantly different ( $P < 0.5$ ), while compared with the model group, the HA-MTX-Lipo MNs and MTX iv were significantly different ( $P < 0.0001$ ). These results indicated that the two groups could inhibit the development of psoriasis and reduce the degree of skin erythema, scaling, and thickening. As can be seen from the body weight changes of mice in Fig. 7(A), except that the body weight of mice in the model group fluctuated greatly, the body weight of mice in other groups was basically in the range of 19–22 g. The spleen is the largest organ in the immune system, and a

higher spleen index indicates a stronger immune response. MTX, as an immunosuppressive agent, can antagonize the stimulatory effect of IMQ on the immune system, and the decrease in the spleen index represents the result of MTX treatment to a certain extent. Fig. 7(B) showed that the spleen index of the model group was about 2.66 times higher than that of the control group ( $P < 0.0001$ ), indicating a robust immune response in mice after IMQ induction. Compared with the model group, the spleen index of Blank MNs, MTX-Lipo MNs, and MTX iv groups did not decrease significantly ( $P > 0.05$ ), while MTX MNs, HA-MTX-Lipo MNs, and MTX po groups had inhibitory effects.

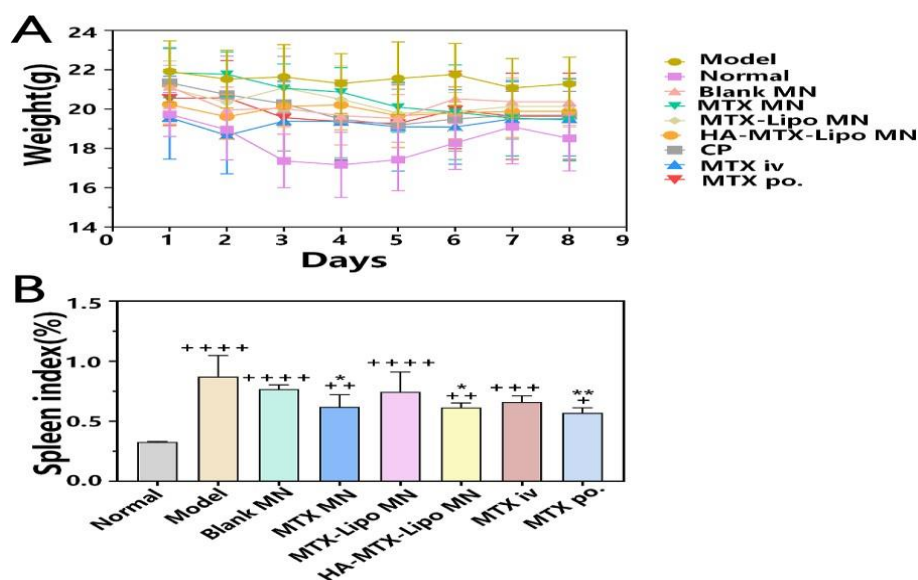


Fig.7. (A) Weight change chart of mice ( $n = 8$ ); (B) Spleen index in mice at day 8 ( $n = 4$ ).

### Pathological changes of psoriasis mouse model

The main histopathological features of psoriasis are hyperkeratosis or inkeratosis, thickening of the spinous layer, thinning of the granular layer, and infiltration of inflammatory cells in the skin [36, 37]. As shown in Fig. 8(A), the skin tissue structure of mice in the normal group was normal, indicated by arrows: a is the epidermis layer, b is the dermis layer. At c, the cuticle cells were incompletely keratinized, and the over-thick cuticle fell off, forming scales, and the granular layer became thinner or even disappeared; d indicated that the spinous layer is hypertrophic and prominent, greatly increasing the thickness of the epidermis. Compared with the normal group, the epidermis of IMQ-induced

mice was significantly thickened. The epidermal thickening was evident in the model group, Blank MNs, MTX-Lipo MNs, and MTX po. The epidermal thickening was somewhat inhibited by MTX MNs and CP groups. The best treatment effect was HA-MTX-Lipo MNs and MTX iv group. The proliferation of epidermal cells was effectively inhibited, the epidermal thickness was thinner, and the skin structure was intact. H&E slices were analyzed and processed by Image J software to measure the epidermal thickness of the psoriasis mouse model. As shown in Fig. 8(B), the epidermal thickness of the control group was about 18.20  $\mu\text{m}$ , and that of the model group was about 97.23  $\mu\text{m}$ , 5.34 times that of the control group, and there was



a significant difference ( $P < 0.0001$ ). After the treatment of HA-MTX-Lipo MNs and MTX iv group, the epidermal thickening was improved to 56.05  $\mu\text{m}$

and 65.09  $\mu\text{m}$ , respectively. There was a significant difference with the model group; the P values were less than 0.001 and 0.01, respectively.

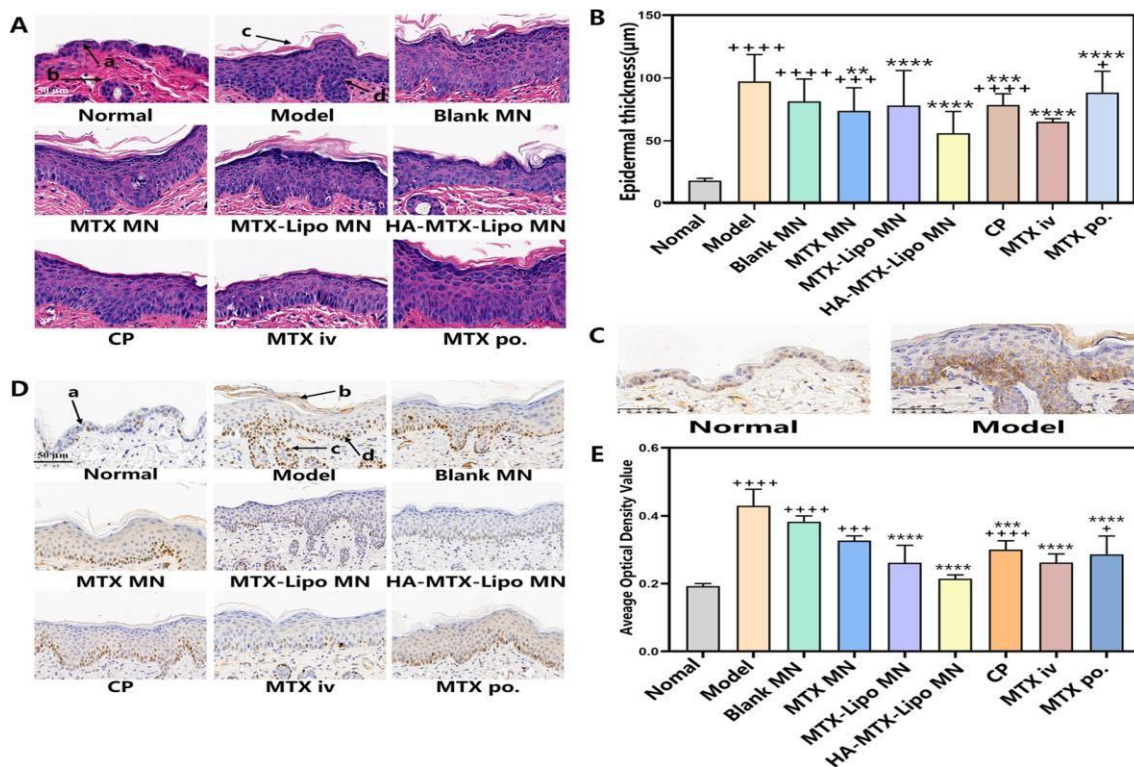


**Fig. 8.** (A) H&E sections of skin of psoriasis mice model treated with different formulations (Scale bar: 50  $\mu\text{m}$ ); (B) Epidermal thickness of skin in a mice model of psoriasis ( $n = 6$ ); (C) Immunohistochemical (CD44) micrographs of the skin of normal mice and mice after IMQ modeling (Scale bar: 50  $\mu\text{m}$ ); (D) Immunohistochemical (Ki67) micrographs of skin of psoriasis mice model treated with different formulations (Scale bar: 50  $\mu\text{m}$ ); (E) The effect of each preparation on the expression level of Ki67 in the skin of a psoriasis mice model ( $n = 4$ ).

These results indicated that HA microneedles delivery of HA-MTX-Lipo can improve the increase of mouse epidermal thickness, and achieve similar results to MTX injection, and the therapeutic effect was good. CD44 is widely expressed on the surface of mammalian cells. It plays a vital role in cell-cell and cell-matrix interactions, such as cell migration, adhesion, proliferation, hematopoiesis, homing, extravasation and lymphocyte activation. CD44 is the primary cell-surface receptor for HA, and HA-CD44 interactions play essential roles in development, inflammation, T-cell aggregation and activation, and tumor growth and metastasis. To verify the expression of CD44 in psoriasis-like skin by immunohistochemistry of CD44 in mouse model skin. It can be seen from Fig. 8 (C) that CD44 expression was low in the skin of normal mice,

but apparent brown deposition can be seen at the arrow after IMQ modeling. CD44 expression was increased in cells at sites of inflammation. As the primary cell surface receptor for HA, CD44 makes more HA-modified HA-MTX-Lipo tend to the inflammatory sites where CD44 is increased, thus acting as MTX. The nuclear antigen present in proliferating cells can be recognized by the expression of Ki67, which reflects the proliferation rate of keratinocytes. As seen from Fig. 8 (D), arrow a referred to the epidermis of the control group, without evident abnormal proliferation of keratinocytes. In contrast, cuticle shedding (arrow b) and cell proliferation were evident in the prominent basal layer (arrows at c and d) in the model group. After IMQ modeling, the epidermal layer of the other groups was significantly thickened and the cell proliferation in



the basal layer was increased considerably, and due to the continuous proliferation of basal cells, the spinous layer was formed, which protruded down to the dermis. The optical density values were analyzed and processed by ImageJ software. Fig. 8(E) was the result of the effect of each preparation on the Ki67 expression level in the skin of the psoriasis mouse model obtained by semi-quantitative analysis. The model group Ki67 expression level higher than the control group significantly ( $P < 0.0001$ ), but there was no significant difference between the MTX-Lipo, HA-MTX-Lipo MNs, and MTX iv groups and the control group ( $P > 0.05$ ). Compared with the model group, the expression level of Ki67 in HA-MTX-Lipo MNs and MTX iv groups was significantly decreased ( $P < 0.0001$ ), and the expression level of Ki67 in CP group was also reduced ( $P < 0.001$ ). The experimental results showed that IMQ ointment caused the continuous proliferation of basal layer cells, formed a prominent spinous layer, thus thickening the skin of mice, and led to the incomplete differentiation of keratinocytes, the peeling of the cuticle, and the formation of scales. After treatment with MTX-Lipo, HA-MTX-Lipo MNs, and MTX iv, the expression level of Ki67 was significantly reduced and the excessive proliferation of epidermal cells was inhibited in psoriasis mouse model. This is due to the MNs and injection administration, the bioavailability of MTX was improved, and the therapeutic effect of MTX is better played. However,

the HA-modified MTX liposomes can remain in the inflammatory skin for longer, causing the internalization of MTX and giving full play to the therapeutic effect of MTX.

### Changes in skin inflammatory cytokines

The pathogenesis and development of psoriasis are closely related to proinflammatory cytokines. The excessive proliferation of keratinocytes can be induced by various proinflammatory cytokines, such as TNF- $\alpha$ , IL-17, and IL-22. At the same time, the inflammatory response is further exacerbated by antimicrobial peptides, cytokines, and chemokines secreted by keratinocytes. Fig. 9 showed that after IMQ ointment treatment, the relative mRNA levels of proinflammatory cytokines, including IL-1 $\beta$ , IL-6, IL-17A, IL-23, and TNF- $\alpha$ , were found to be substantial increased in the skin of the mouse psoriasis model ( $P < 0.0001$ ). Cytokine mRNA levels were significantly down-regulated in each groups compared with model groups (except the blank MNs group). The down-regulation ability of HA-MTX-Lipo MNs group and MTX iv group was the most prominent, and the relative mRNA levels of TNF- $\alpha$ , IL-23, and IL-6 were not significantly different from those of the control group ( $P > 0.05$ ). In conclusion, the mRNA levels of proinflammatory cytokines can be effectively reduced by HA-MTX-Lipo MNs in IMQ-induced psoriasis animal models.

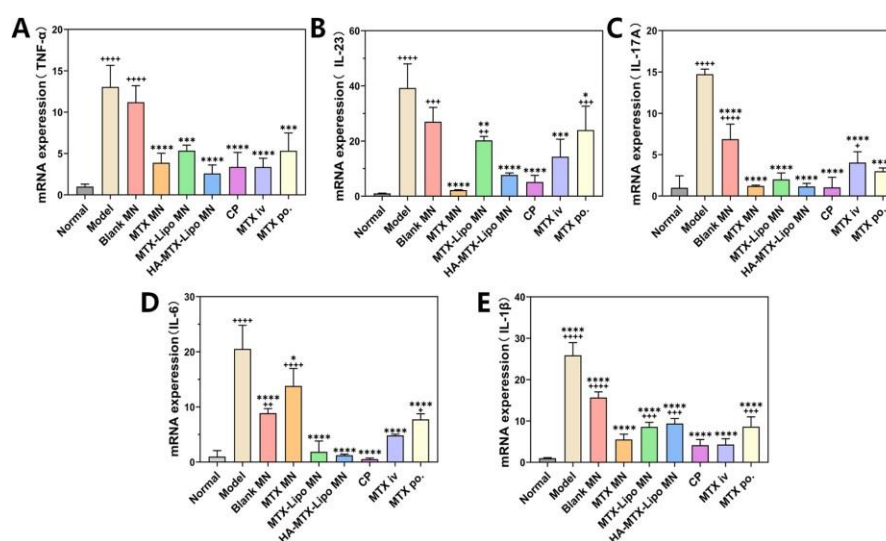


**Fig. 9.** Effects of different preparations on the expression levels of TNF- $\alpha$ , IL-23, IL-17A, IL-6 and IL-1 $\beta$  in mice skin after IMQ modeling ( $n = 3$ ).



#### 4. Conclusions

In summary, we have developed an MTX-loaded liposome with HA surface modification, which could be transdermally delivered by MNs, taking full advantage of the enhanced pore-forming permeability of MNs, while retaining the properties of liposomes for controlled release, targeting, and drug protection. The HA-MTX-Lipo had uniform size, good dispersion, and sufficient stability. Moreover, the prepared MNs had adequate mechanical properties and negligible skin irritation. The *in vitro* and *in vivo* studies demonstrated that the HA-MTX-Lipo MNs could inhibit HaCaT cells, the expression of inflammatory cytokines, and the excessive proliferation of the epidermal cells. We also found that the HAMTX-Lipo MNs could inhibit the development of psoriasis, and reduce the skin erythema, scaling and thickening. Taken together, HA-MTX-Lipo MNs is an efficient local drug delivery platform, which can avoid systemic toxicity of MTX, achieve a good therapeutic effect, and enable a potential alternative therapy for psoriasis. At the same time, this study has not yet explored the process of interaction between HA and CD44 *in vivo* and the mechanism of inhibition of pro-inflammatory cytokines by this system, and there are still problems with low drug loading capacity of microneedles. Therefore, further research will be conducted on these issues in the future.

#### Declaration of competing interest

The author declares no conflict of interest, financial or otherwise.

#### Acknowledgements

This research did not receive any specific grant from funding agencies in the public, commercial, or not-for-profit sectors. The authors are helpful to the National Institute of Technology (NIT), Rourkela, Odisha, India for providing all required facilities. The authors would also like to thank to Columbia Institute of Pharmacy, Raipur, Chhattisgarh, India for providing laboratory animal facilities.

#### References

- [1] Aghaei, H., Nazar, A.R.S., Varshosaz, J., 2021. Double flow focusing microfluidic-assisted based preparation of methotrexate-loaded liposomal nanoparticles: encapsulation efficacy, drug release and stability. *Colloids Surfaces a-Physicochem. Eng. Aspects* 614.
- [2] Amarji, B., Garg, N.K., Singh, B., Katare, O.P., 2016. Microemulsions mediated effective delivery of methotrexate hydrogel: more than a tour de force in psoriasis therapeutics. *J. Drug Target.* 24 (2), 147–160.
- [3] Armstrong, A.W., Read, C., 2020. Pathophysiology, clinical presentation, and treatment of psoriasis: a review. *JAMA* 323 (19), 1945–1960.
- [4] Bi, D., Qu, F., Xiao, W., Wu, J., Liu, P., Du, H., Xie, Y., Liu, H., Zhang, L., Tao, J., Liu, Y., Zhu, J., 2023. Reactive oxygen species-responsive gel-based microneedle patches for prolonged and intelligent psoriasis management. *ACS Nano* 17 (5), 4346–4357.
- [5] Cai, Y., Shen, X., Ding, C., Qi, C., Li, K., Li, X., Jala, Venkatakrishna R., Zhang, H.-g., Wang, T., Zheng, J., Yan, J., 2011. Pivotal role of dermal IL-17-producing  $\gamma\delta$  T cells in skin inflammation. *Immunity* 35 (4), 596–610.
- [6] Chen, Z., 2018. What's new about the mechanism of methotrexate action in psoriasis? *Br. J. Dermatol.* 179 (4), 818–819.
- [7] Cronstein, B., 2010. How does methotrexate suppress inflammation. *Clin. Exp. Rheumatol.* 28, S21–S23, 5 Suppl 61.
- [8] Du, H., Liu, P., Zhu, J., Lan, J., Li, Y., Zhang, L., Zhu, J., Tao, J., 2019. Hyaluronic acidbased dissolving microneedle patch loaded with methotrexate for improved treatment of psoriasis. *ACS Appl. Mater. Interfaces* 11 (46), 43588–43598.
- [9] Duarah, S., Sharma, M., Wen, J., 2019. Recent advances in microneedle-based drug delivery: special emphasis on its use in paediatric population. *Eur. J. Pharmaceut. Biopharmaceut.* 136, 48–69.
- [10] Fratoddi, I., Benassi, L., Botti, E., Vaschieri, C., Venditti, I., Bessar, H., Samir, M.A., Azzoni, P., Magnoni, C., Costanzo, A., Casagrande, V., Federici, M., Bianchi, L., Pellacani, G., 2019. Effects of topical methotrexate loaded gold nanoparticle in cutaneous inflammatory mouse model. *Nanomedicine: Nanotechnol., Biol. Med.* 17, 276–286.
- [11] Griffiths, C., Armstrong, A., Gudjonsson, J., Barker, J., 2021. Psoriasis. *Lancet* 397 (10281), 1301–1315.
- [12] Griffiths, C.E.M., Barker, J.N.W.N., 2007. Psoriasis 1 - Pathogenesis and clinical features of psoriasis. *Lancet* 370 (9583), 263–271.
- [13] Guimaraes, D., Cavaco-Paulo, A., Nogueira, E., 2021. Design of liposomes as drug delivery



- system for therapeutic applications. *Int. J. Pharm.* 601.
- [14] Hackethal, J., Iredahl, F., Henricson, J., Anderson, C.D., Tesselaar, E., 2021. Microvascular effects of microneedle application. *Skin Res. Technol.* 27 (2), 121–125.
- [15] Hoekstra, M., Haagsma, C., Neef, C., Proost, J., Knuif, A., van de Laar, M., 2006. Splitting high-dose oral methotrexate improves bioavailability: a pharmacokinetic study in patients with rheumatoid arthritis. *J. Rheumatol.* 33 (3), 481–485.
- [16] Jiang, W.Y., Chattedee, A.D., Raychaudhuri, S.P., Raychaudhuri, S.K., Farber, E.M., 2001. Mast cell density and IL-8 expression in nonlesional and lesional psoriatic skin. *Int. J. Dermatol.* 40 (11), 699–703.
- [17] Jordan, A.R., Racine, R.R., Hennig, M.J.P., Lokeshwar, V.B., 2015. The role of CD44 in disease pathophysiology and targeted treatment. *Front. Immunol.* 6, 182–182.
- [18] Kotla, N.G., Bonam, S.R., Rasala, S., Wankar, J., Bohara, R.A., Bayry, J., Rochev, Y., Pandit, A., 2021. Recent advances and prospects of hyaluronan as a multifunctional therapeutic system. *J. Controlled Release* 336, 598–620.
- [19] Large, D.E., Abdelmessih, R.G., Fink, E.A., Auguste, D.T., 2021. Liposome composition in drug delivery design, synthesis, characterization, and clinical application. *Adv. Drug Deliv. Rev.* 176.
- [20] Lowes, M.A., Suarez-Farinas, M., Krueger, J.G., 2014. Immunology of psoriasis. *Annu. Rev. Immunol.* 32, 227–255.
- [21] Mathers, A.R., Larregina, A.T., 2006. Professional antigen-presenting cells of the skin. *Immunol. Res.* 36 (1), 127–136.
- [22] Menting, S.P., Dekker, P.M., Limpens, J., Hooft, L., Spuls, P.I., 2016. Methotrexate dosing regimen for plaque-type psoriasis: a systematic review of the use of test-dose, startdose, dosing scheme, dose adjustments, maximum dose and folic acid supplementation. *Acta Derm. Venereol.* 96 (1), 23–29.
- [23] Ngo, M.A., Maibach, H.I., 2010. Dermatotoxicology: historical perspective and advances. *Toxicol. Appl. Pharmacol.* 243 (2), 225–238.
- [24] Olatunji, O., Das, D.B., Garland, M.J., Belaid, L., Donnelly, R.F., 2013. Influence of array interspacing on the force required for successful microneedle skin penetration: theoretical and practical approaches. *J. Pharm. Sci.* 102 (4), 1209–1221.
- [25] Ponta, H., Sherman, L., Herrlich, P.A., 2003. CD44: from adhesion molecules to signalling regulators. *Nature Rev. Molec. Cell Biol.* 4 (1), 33–45.
- [26] Pradhan, M., Alexander, A., Singh, M.R., Singh, D., Saraf, S., Saraf, S., Ajazuddin, 2018. Understanding the prospective of nano-formulations towards the treatment of psoriasis. *Biomed. Pharmacother.* 107, 447–463.
- [27] Puigdemont, A., Brazís, P., Ordeix, L., Dalmau, A., Fuertes, E., Olivar, A., Pérez, C., Ravera, I., 2013. Efficacy of a new topical cyclosporine A formulation in the treatment of atopic dermatitis in dogs. *Veterinary J.* 197 (2), 280–285.
- [28] Rahman, M., Akhter, S., Ahmad, J., Ahmad, M.Z., Beg, S., Ahmad, F.J., 2015. Nanomedicine-based drug targeting for psoriasis: potentials and emerging trends in nanoscale pharmacotherapy. *Expert Opin. Drug Deliv.* 12 (4), 635–652.
- [29] Ranganathan, P., McLeod, H.L., 2006. Methotrexate pharmacogenetics: the first step toward individualized therapy in rheumatoid arthritis. *Arthritis & Rheumatism: Official J. Am. College Rheumatol.* 54 (5), 1366–1377.
- [30] Rendon, A., Schakel, K., 2019. Psoriasis Pathogenesis and Treatment. *Int. J. Mol. Sci.* 20 (6), 1475.
- [31] Ruan, S., Zhang, Y., Feng, N., 2021. Microneedle-mediated transdermal nanodelivery systems: a review. *Biomater. Sci.* 9 (24), 8065–8089.
- [32] Saporito, F.C., Menter, M.A., 2004. Methotrexate and psoriasis in the era of new biologic agents. *J. Am. Acad. Dermatol.* 50 (2), 301–309.
- [33] Stern, R., Asari, A.A., Sugahara, K.N., 2006. Hyaluronan fragments: an information-rich system. *Eur. J. Cell Biol.* 85 (8), 699–715.
- [34] Tekko, I.A., Permana, A.D., Vora, L., Hatahet, T., McCarthy, H.O., Donnelly, R.F., 2020. Localised and sustained intradermal delivery of methotrexate using nanocrystal-loaded microneedle arrays: potential for enhanced treatment of psoriasis. *Eur. J. Pharmaceut. Sci.* 152, 105469.
- [35] Xu, H., Paxton, J., Lim, J., Li, Y., Zhang, W., Duxfield, L., Wu, Z., 2014. Development of high-content gemcitabine pegylated liposomes and their cytotoxicity on drug-resistant pancreatic tumour cells. *Pharm. Res.* 31 (10), 2583–2592.
- [36] Yang, X., Tang, Y., Wang, M., Wang, Y., Wang, W., Pang, M., Xu, Y., 2021. Co-delivery of methotrexate and nicotinamide by cerosomes for topical psoriasis treatment with enhanced efficacy. *Int. J. Pharm.* 605, 120826.



- [37] Zaba, L.C., Cardinale, I., Gilleaudeau, P., Sullivan-Whalen, M., Suárez-Farinas, M., Fuentes-Duculan, J., Novitskaya, I., Khatcherian, A., Bluth, M.J., Lowes, M.A., 2007. Amelioration of epidermal hyperplasia by TNF inhibition is associated with reduced Th17 responses. *J. Exp. Med.* 204 (13), 3183–3194.
- [38] Zhou, Y., Yang, L., Lyu, Y., Wu, D., Zhu, Y., Li, J., Jiang, D., Xin, X., Yin, L., 2023. Topical delivery of ROS-responsive methotrexate prodrug nanoassemblies by a dissolvable microneedle patch for psoriasis therapy. *Int. J. Nanomed.* 18, 899–915.